SUPPLEMENTARY INFORMATION

Synergistic Bimetallic MOF-Integrated MXene Nanosheets for Enhanced Catalytic Degradation of Carbamazepine and Hydrogen Production: A Dual-Functional Approach for Water Remediation and Energy Applications

Van-Anh Thai [a,#], Thanh-Binh Nguyen [a,#], Chiu-Wen Chen[a, b], Xuan-Thanh Bui[c, d], Ruey-an Doong[e], Cheng-Di Dong[a, b*]

a. Institute of Aquatic Science and Technology, National Kaohsiung University of Science and Technology, Kaohsiung City, 81157, Taiwan.

b. Department of Marine Environmental Engineering, National Kaohsiung University of Science and Technology, Kaohsiung City, 81157, Taiwan.

c. Key Laboratory of Advanced Waste Treatment Technology, Ho Chi Minh City University of Technology (HCMUT), Vietnam National University Ho Chi Minh (VNU-HCM), Thu Duc city, Ho Chi Minh City 700000, Viet Nam.

d. Faculty of Environment and Natural Resources, Ho Chi Minh City University of Technology (HCMUT), 268 Ly Thuong Kiet Street, District 10, Ho Chi Minh City 700000, Viet Nam.

e. Institute of Analytical and Environmental Sciences, National Tsing Hua University, Hsinchu, 30013, Taiwan

[#] Contributed equally

*Corresponding author.

Email: cddong@nkust.edu.tw (Cheng-Di Dong)

S1. Reagent

The chemicals used in this study include cobalt nitrate, 6-hydrate (98%, $Co(NO_3)_2.6H_2O$, J.T. Baker, United Kingdom), Ferrous(II) sulfate hexahydrate ($FeSO_4.6H_2O$, 98%) (Sigma-Aldrich, USA), 2-methylimidazole (99%, $C_4H_6N_2$, Sigma-Aldrich, India), methyl alcohol (99.9%, CH_3OH, Macron, USA), Carbamazepine (98%, $C_{15}H_{12}N_2O$, Sigma-Aldrich, China), deuterium oxide (99.9 atom % D, Sigma-Aldrich, Canada), MXene ($Ti_2Al_3C_2$, 99.5%), 1,3,5-benzene tricarboxylic acid (BTC, $C_9H_6O_6$, 98%) and Oxone®potassium peroxymonosulfate ($KHSO_5.0.5KHSO_4.0.5K_2SO_4$, Sigma-Aldrich, USA). Deionized water (DIW) used in this study was obtained from a Millipore®Synergy® system with a resistivity of less than 18 MΩ-cm.

S2. Characterization of materials

The crystal structure of materials was determined by the X-ray diffraction method and performed on a D8 Advance diffractometer, Bruker, Germany, with Cu Kα radiation (λ = 0.154 nm and angle scanning range of 5-85^o). The morphology of materials was imaged by JSM-7800 Schottky FESEM (field emission scanning electron microscope), JEOL, the USA and F20 G2 MAT S-TWIN TEM (field emission gun transmission electron microscope), Tecnai, FEI Co. Energy-dispersive X-ray spectroscopy (EDS) was performed on Thermo ESCALB 250Xi spectrometer (Waltham, MA, USA) for catalyst elemental composition determination. Micromeritics ASAP 2020 Physisorption (Norcross, GA, USA) was conducted to measure Brunauer-Emmett-Teller (BET), Thermo Nicolet^{TM} iS10^{TM} -FTIR spectrometer (USA) determined the Fourier transform infrared (FTIR) spectra of composites. In 30-1000 ^{o}C temperature range, thermo gravimetric analysis (TGA) and differential scanning calorimetry (DSC) were conducted by a Mettler-Toledo TGA/DSC 3+ STAR (Schwerzenbach, Switzerland) at a heating temperature ramping rate of 10°C min^{-1} in the temperature range of 30−1000 °C under air atmosphere. Bruker EMXplust-10/12/P/L spectrometer (Bruker, Bremen, Germany) measured Electron paramagnetic resonance (EPR) at 9.85 GHz and power of 22.8 mW.

S3. Chemical analysis

The concentration of CBZ was performed on the high-performance liquid chromatography (Hitachi HPLC Chromaster) with an ultraviolet (UV) detector at a wavelength of 286 nm. The mobile phase consisted of methanol and 0.1% formic acid (60:40, v/v), with a flow rate of 1 mL min-1 and an injection volume of 20 μL. C18 column dimensions are 50 mm x 4.6 mm x 5 μm and run in a temperature controller of 35 C. ICP-MS (Inductively coupled plasma mass spectrometry, Agilent 7500a, Santa Clara, CA USA) were conducted to determine the efficiency of the oxidation process and the concentration of metal leaching in the system. An ultra-high pressure liquid chromatography coupled with a mass spectrometer (UPLC® I-class IVD/Xevo® TQ-S micro IVD, Water Corporation, MA, USA) with an extend C_{18} column (2.1 x 50 mm 1.7 μm) was used to detect the byproducts of CBZ. The mobile phase A was acetonitrile, and the mobile phase B was 0.1% formic acid in H_2O. The gradient elution procedure was 0→1→2→3→6→7→11→12→18 min. The mobile phase A of acetonitrile was 95%→85%→80%→70%→10%→2%→2%→95%. The identification of the intermediates was carried out using the ESI positive ion mode. The source temperature was 150 ^{o}C. The desolvation temperature was 450 ^{o}C, and the sheath gas flow rate was 650 L hr^{-1}. The source voltage was set at 3500 V.

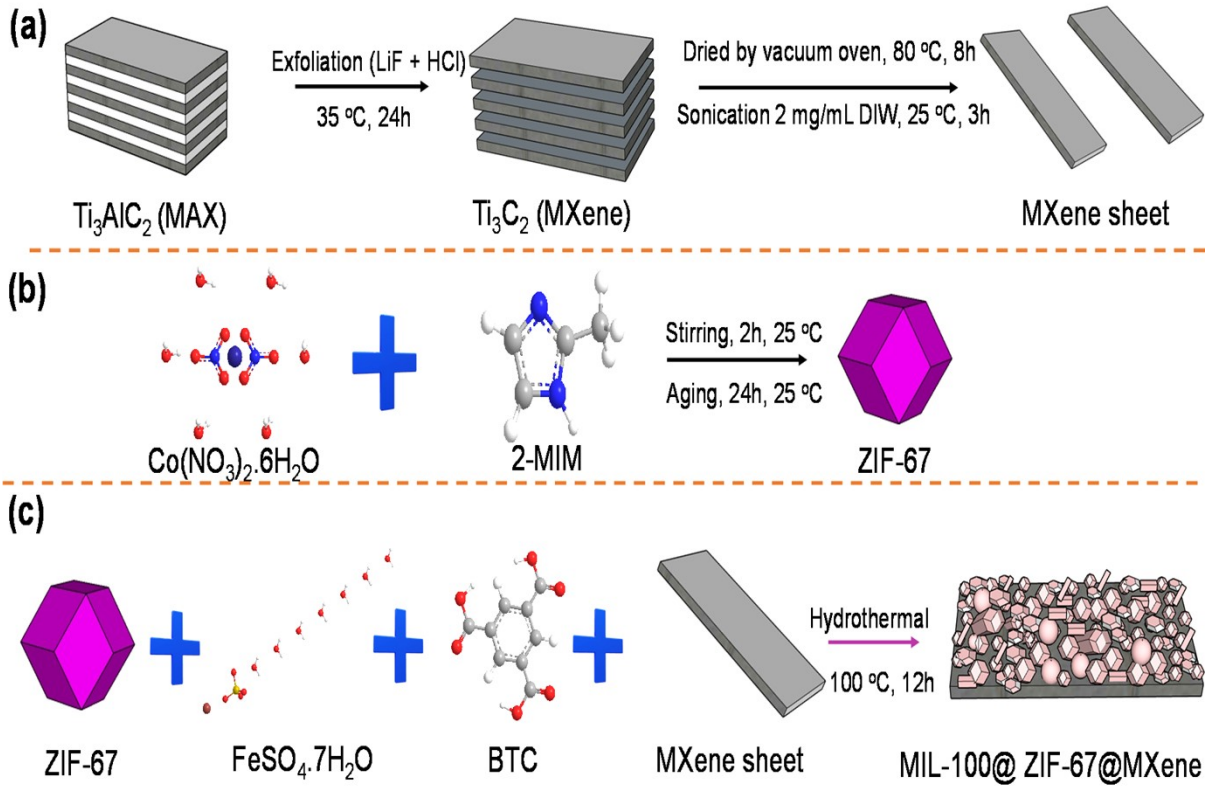

Fig. S1. Synthesis procedure (a) MXene, (b) ZIF-67, and (c) MIL-100@ZIF-67@MXene.

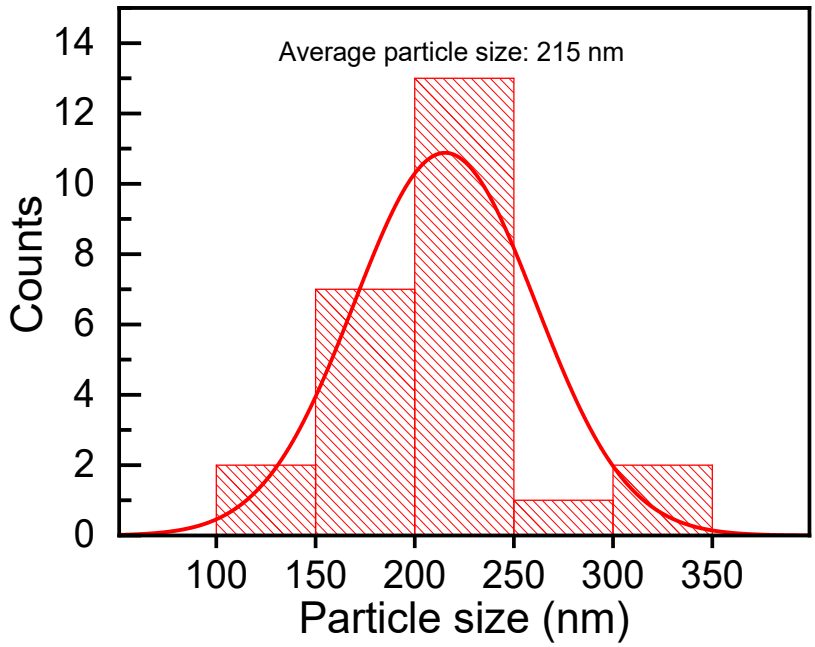

Fig. S2. Size distribution of MIL-100@ZIF-67 on MXene nanosheet.

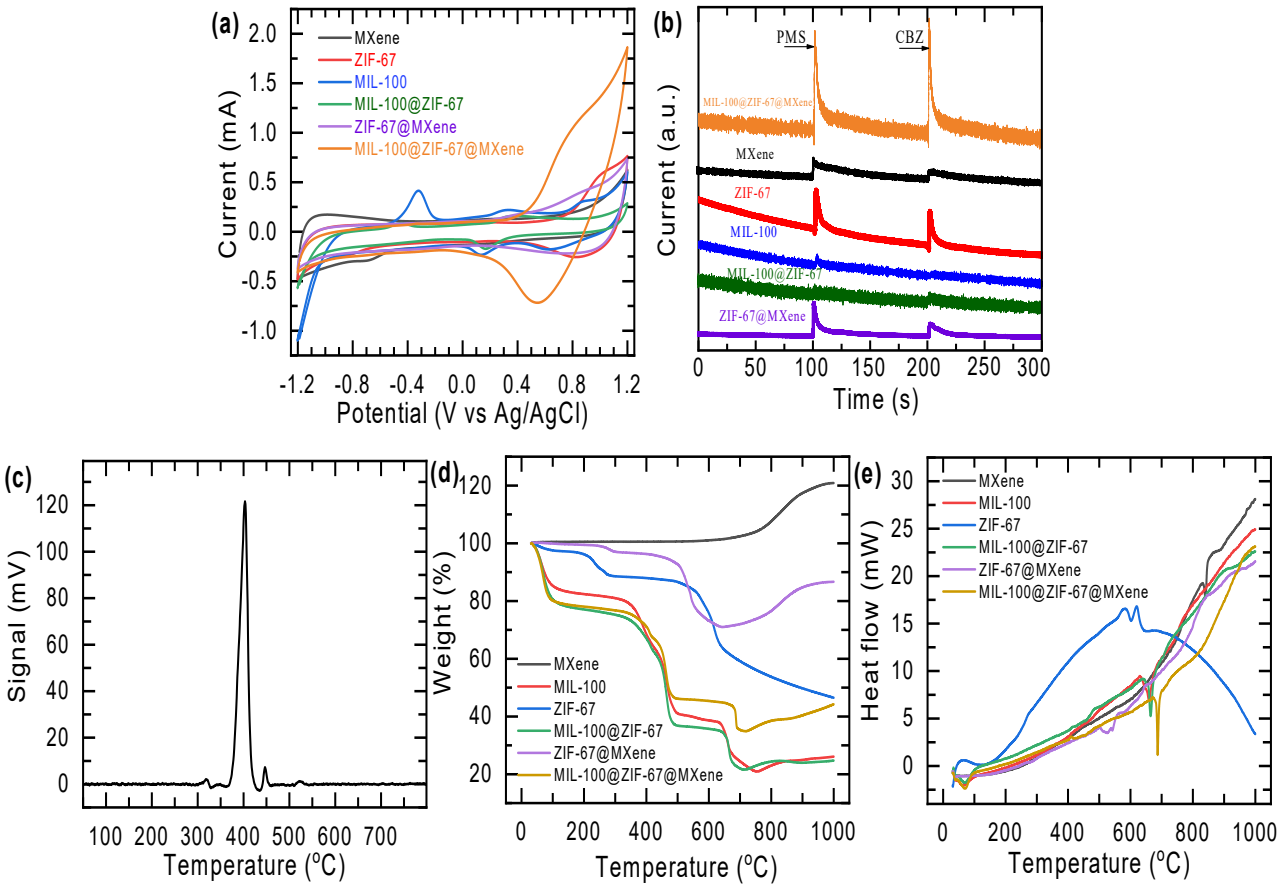

Fig. S3. (a) Cyclic voltammetry, (b) chronoamperometry, (c) H_2-TPD profiles of MIL-100@ZIF-67@MXene, (d) TGA, and (e) DSC plots of as-prepared catalysts.

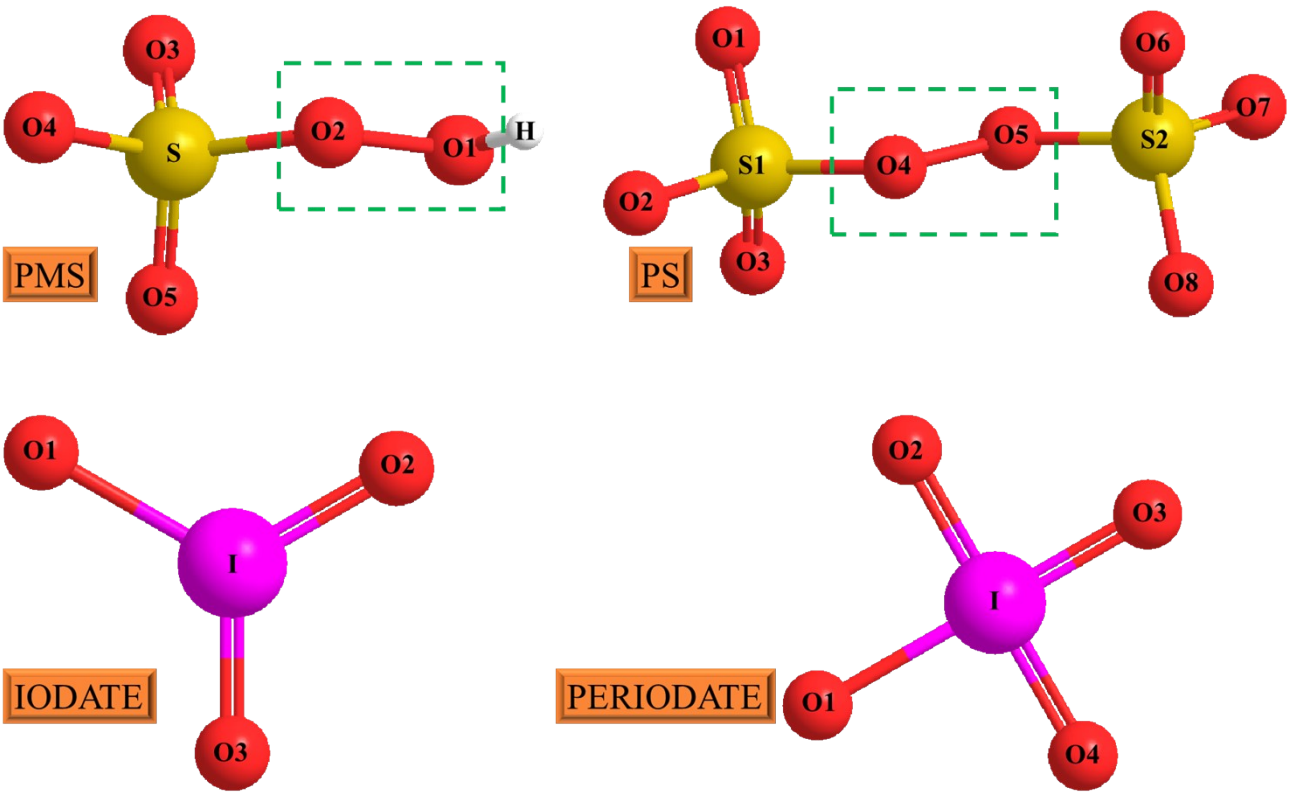

Fig. S4. Chemical structures of oxidizing agents

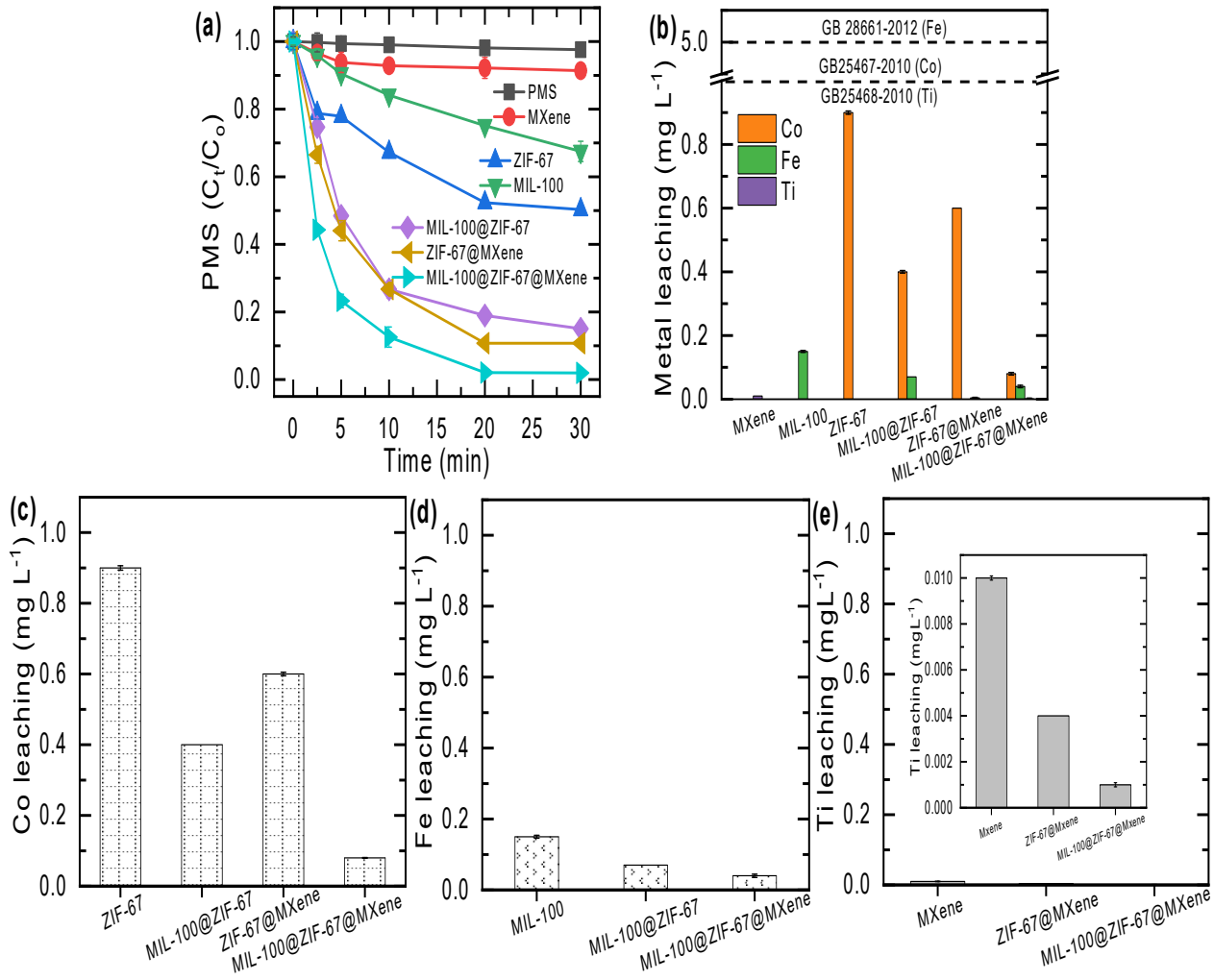

Fig. S5. (a) PMS consumption by the as-prepared catalysts, (b) metal leaching, (c) Co leaching, (d) Fe leaching, and (e) Ti leaching from the as-prepared catalysts after the reaction.

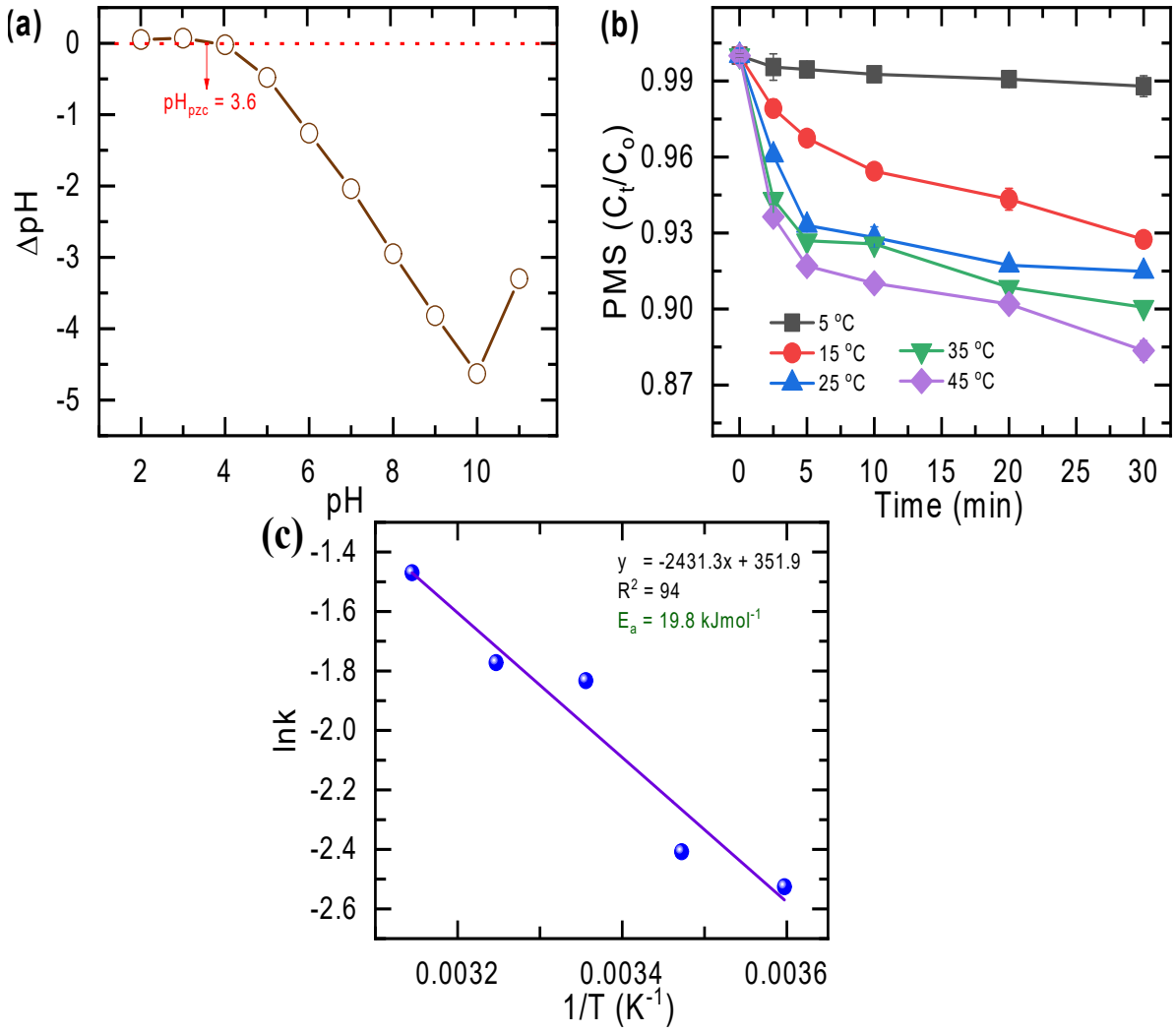

Fig. S6. (a) pH_{pzc} of MIL-100@ZIF-67@MXene, (b) the PMS consumption, and (c) Activation energy at various temperatures.

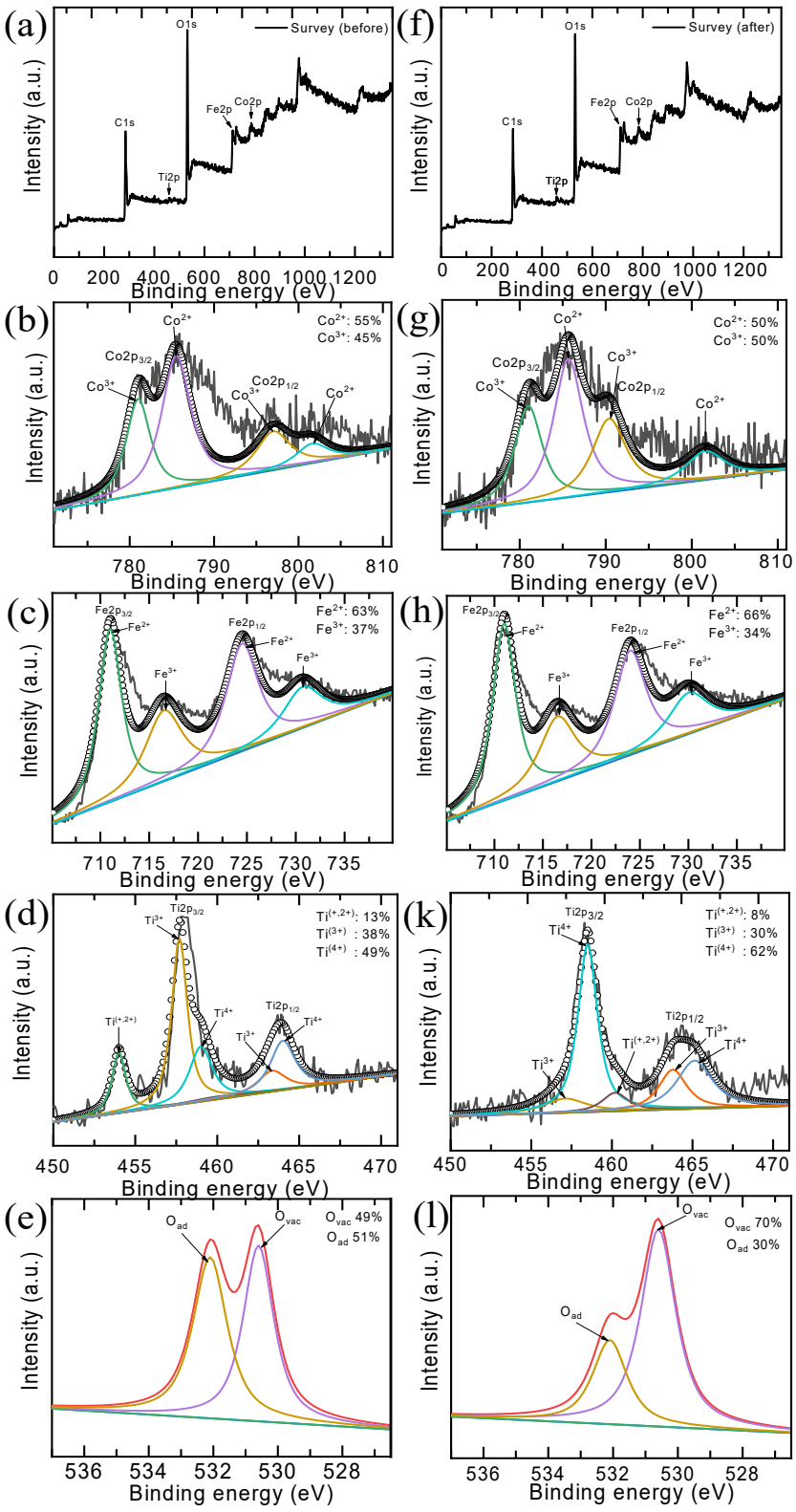

Fig. S7. XPS spectra of (a and f) survey, (b and g) Co2p, (c and h) Fe2p, (d and k) Ti2p, and (e and l) O1s before and after reaction of MIL-100@ZIF-67@MXene.

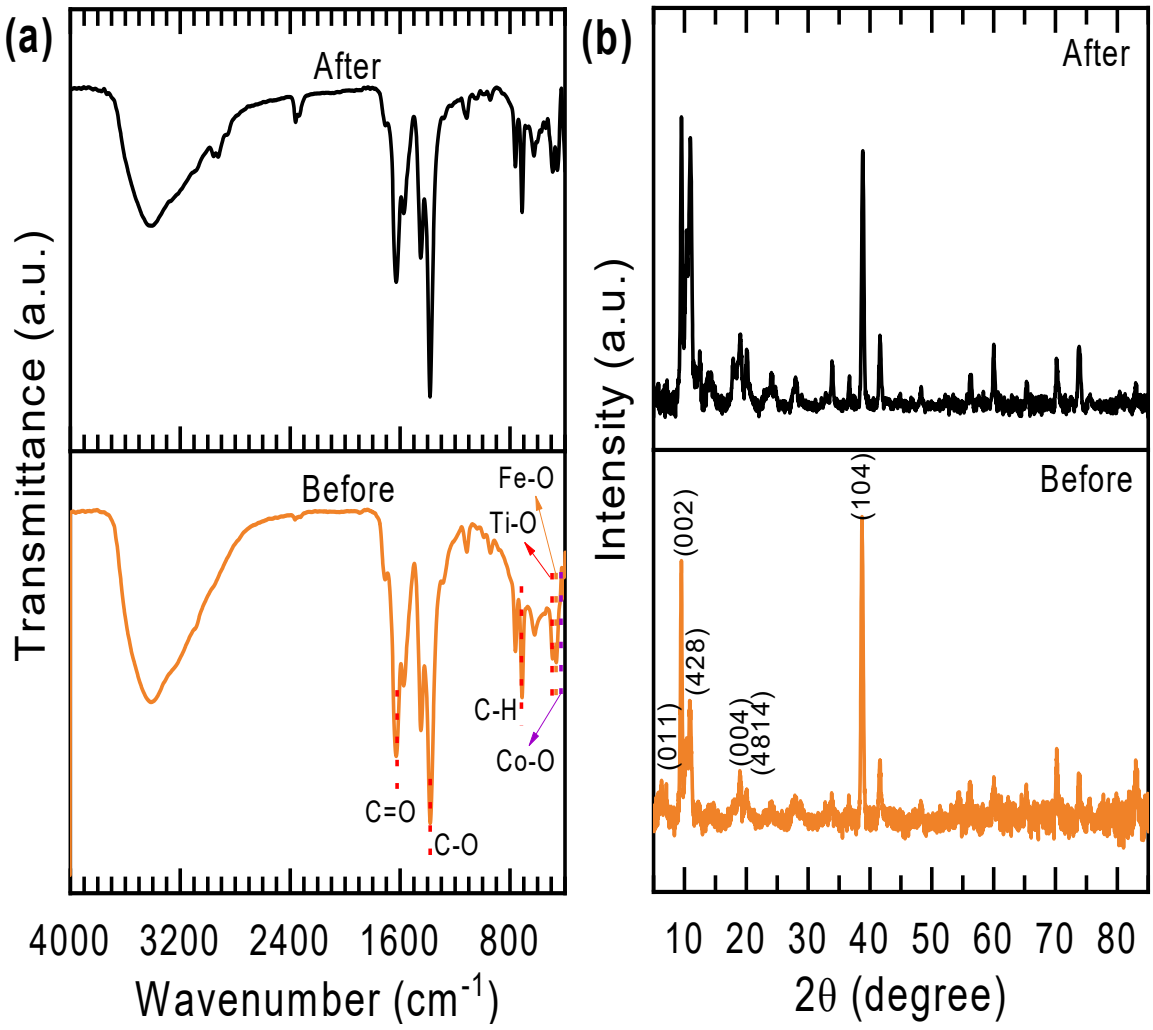

Fig. S8 (a) FTIR, and (b) XRD spectra before and after reaction of MIL-100@ZIF-67@MXene.

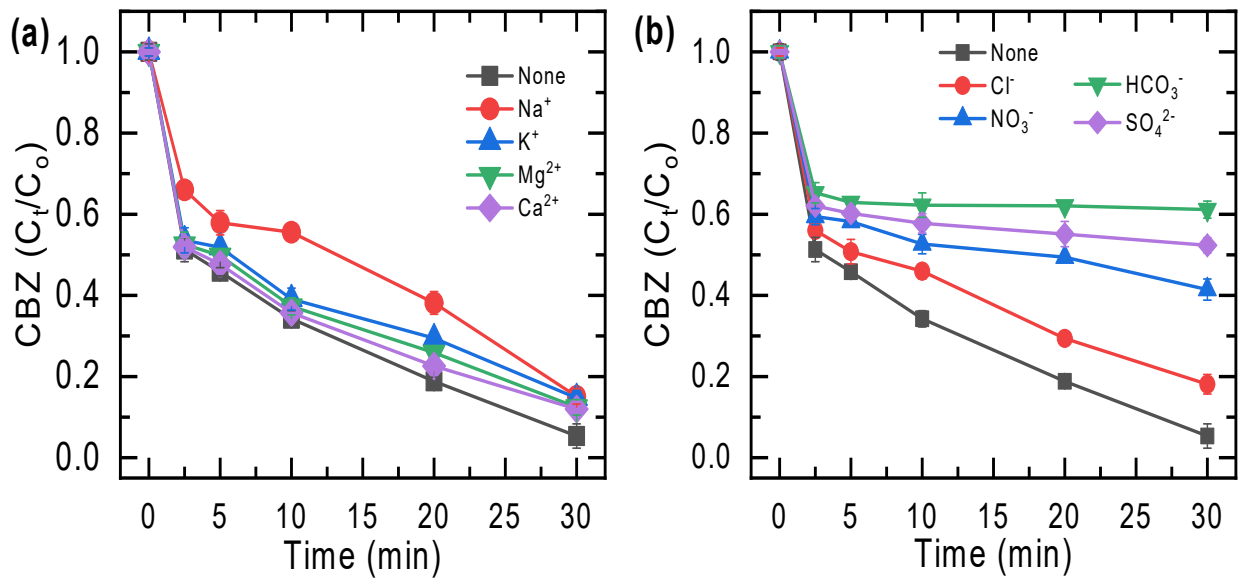

Fig. S9. Effect of (a) cations and (b) anions on CBZ degradation (Experimental condition: [Catalyst] = 50 mg L^{-1}, [PMS] = 0.3 mM, [CBZ] = 0.02 mM, [Ions] = 10 mM, pH = 7, V = 100 mL).

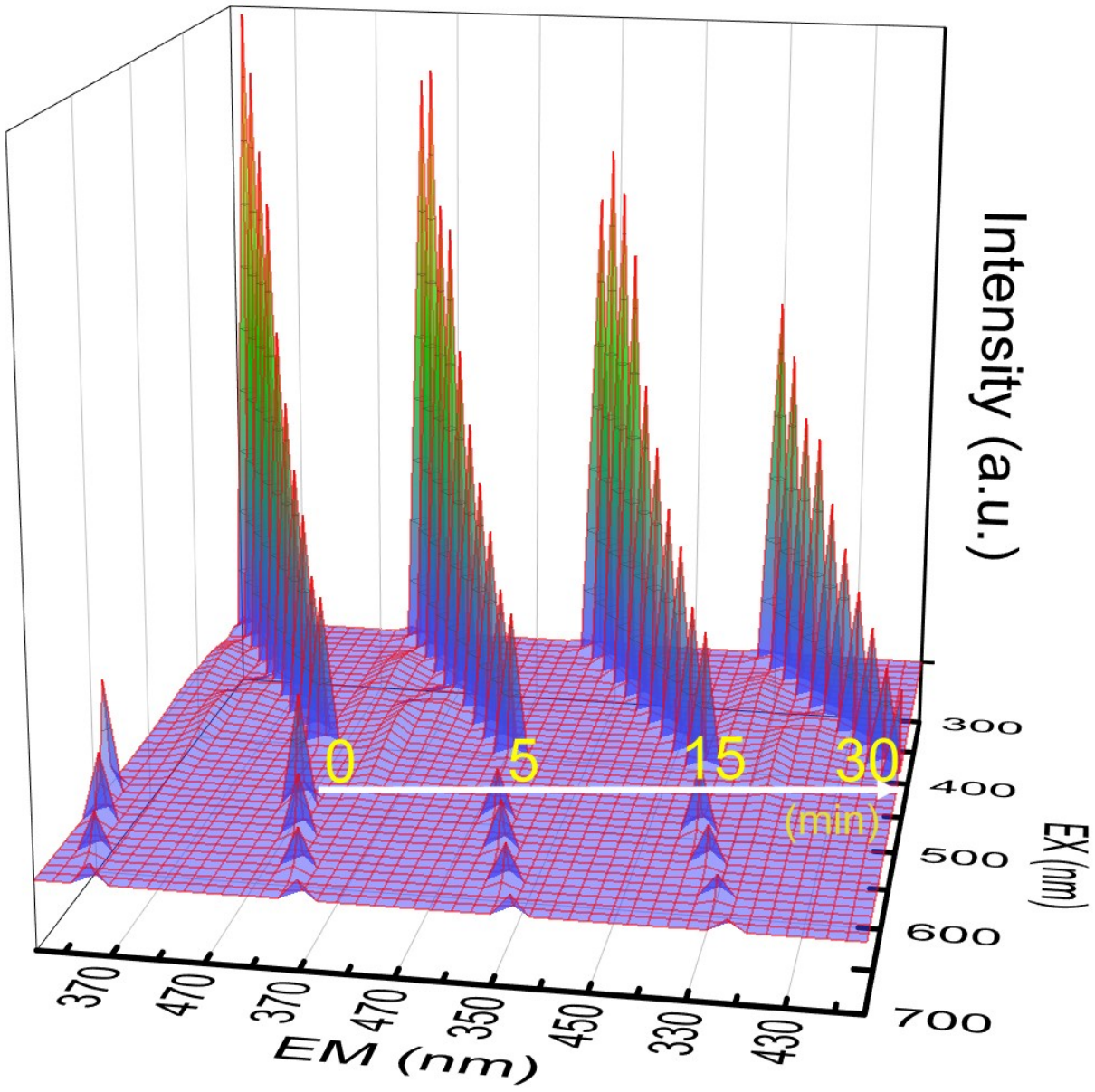

Fig. S10. 3D EEMs of CBZ in MIL-100@ZIF-67@MXene/PMS system after 30 min reaction.

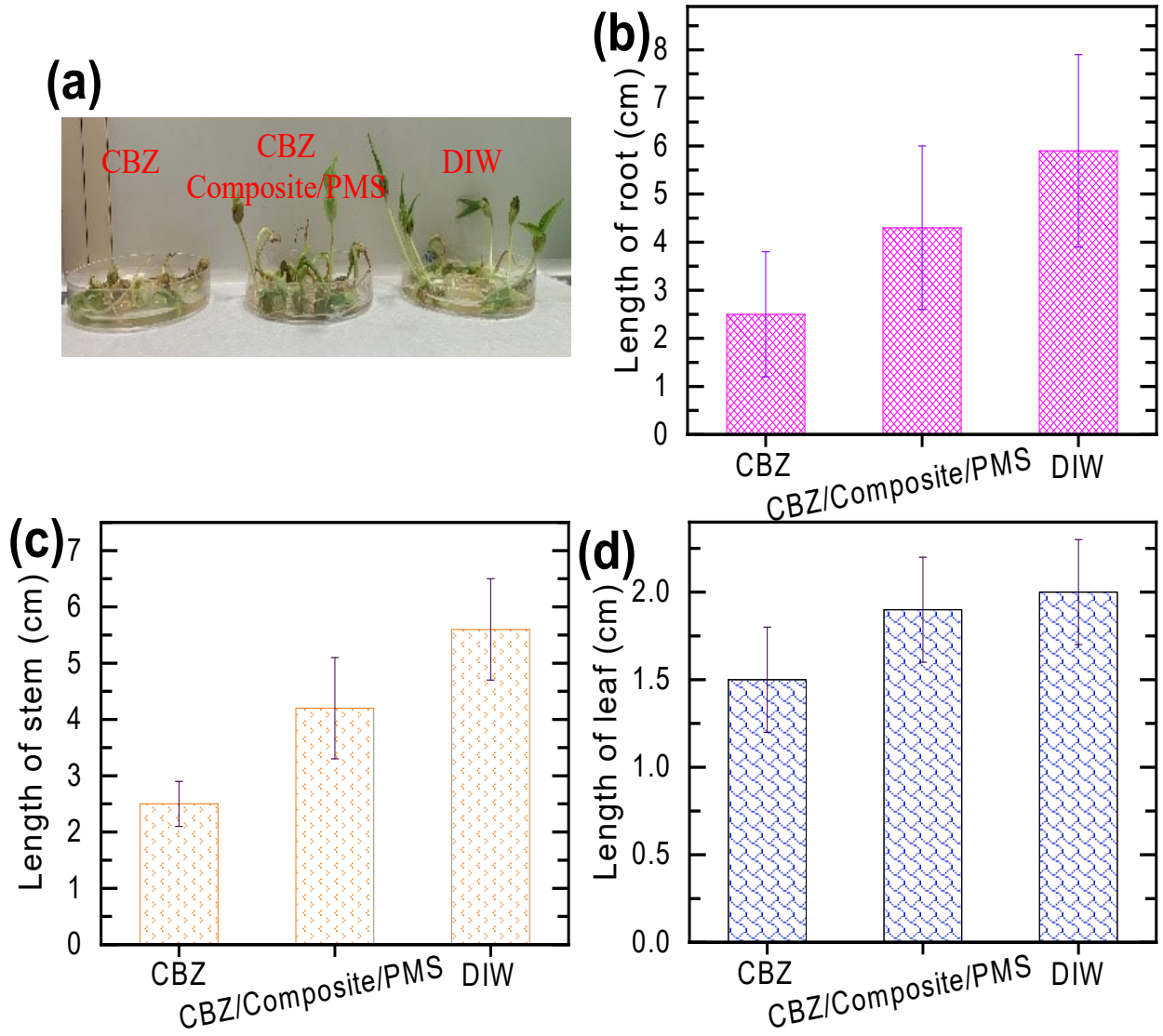

Fig. S11. (a) Growth inhibition, (b) root, (c) stem, and (d) leaf length of mung bean in CBZ, CBZ after treatment, and DIW after seven days.

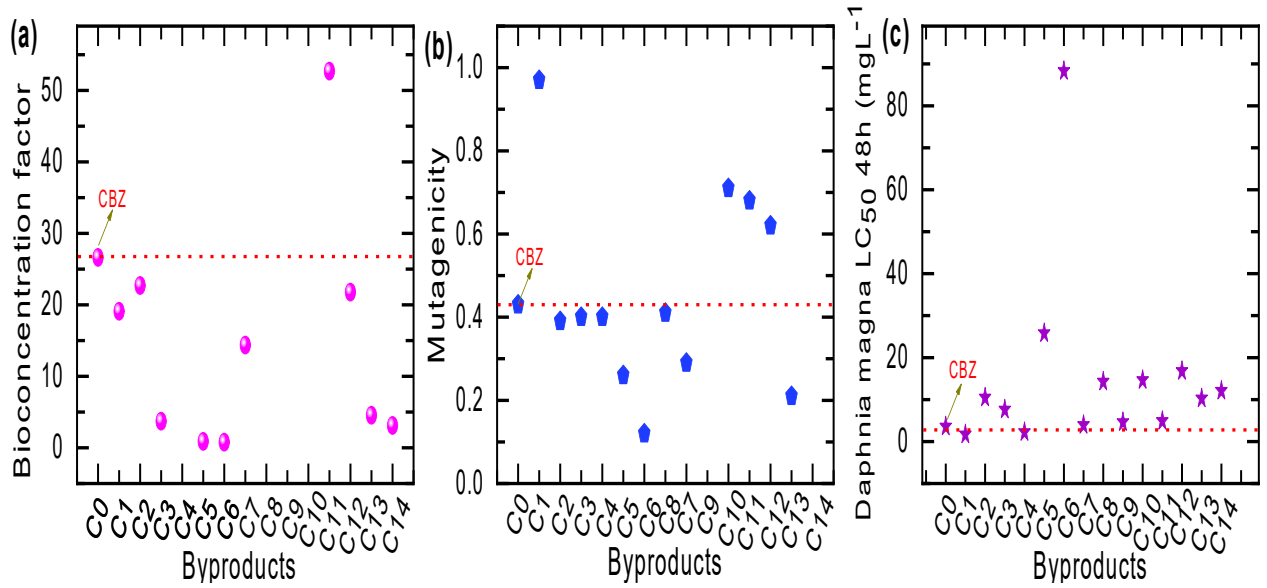

Fig. S12. Toxicity evaluation of CBZ and its degradation byproducts in case of (a) Bioconcentration factor, (b) Mutagenicity, and (c) *Daphnia magna* LC_{50} 48h.

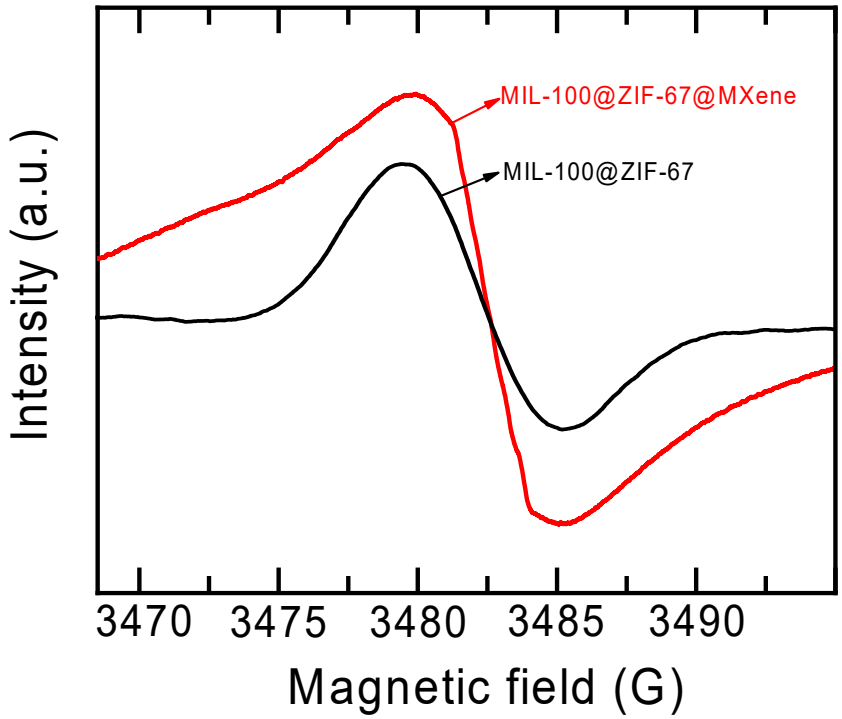

Fig. S13. EPR spectra of O_{defect} in MIL-100@ZIF-67 and MIL-100@ZIF-67@MXene.

Table S1. Fukui function (f^0, f^+, f^-) of PS and PMS.

PS				PMS			
Atom	f^0	f^+	f^-	Atom	f^0	f^+	f^-
O1	0.095	0.077	0.112	O1	0.268	0.293	0.244
O2	0.110	0.113	0.106	O2	0.220	0.214	0.226
O3	0.095	0.075	0.115	O3	0.090	0.077	0.103
O4	0.146	0.177	0.114	O4	0.104	0.104	0.154
O5	0.146	0.178	0.114	O5	0.128	0.128	0.133
O6	0.094	0.077	0.111				
O7	0.109	0.113	0.106				
O8	0.094	0.075	0.114				

Iodate				Periodate			
Atom	f^0	f^+	f^-	Atom	f^0	f^+	f^-
I	0.219	0.038	0.400	I	0.126	-0.050	0.303
O1	0.0144	0.167	0.014	O1	0.209	0.397	0.020
O2	0.098	0.299	0.098	O2	0.150	0.140	0.160
O3	0.310	0.091	0.0310	O3	0.158	0.150	0.166
				O4	0.150	0.140	0.160

Table S2. Comparison of activated energy (Ea) of MIL-100@ZIF-67@MXene and the different catalysts in PMS activation for CBZ degradation.

Catalysts	E_a (kJ mol^{-1})	Ref.
Triple-shelled Co_3O_4	59.0	[1]
Co-SNC	43.9	[2]
Co@NPC-CMB	39.4	[3]
110-α-MnO_2	38.6	[4]
E@MO	26.8	[4]
MIL-100@ZIF-67@MXene	19.8	This study

Table S3. Characteristics of water matrices

Parameters	Unit	Tap water	River water

pH		7.7	8.2
ORP	mV	-69	-89
Conductivity	$\mu S\ cm^{-1}$	595	1380
Salinity	ppt	0.15	0.21
TDS	ppm	242	499
COD	$mgO_2\ L^{-1}$	70	129
Cl^-	$mg\ L^{-1}$	0.035	0.37
SO_4^{2-}	$mg\ L^{-1}$	0.15	0.35
Alkalinity	$mgCO_3\ L^{-1}$	78	97
NO_2^-	$mg\ L^{-1}$	0.002	0.259
NO_3^-	$mg\ L^{-1}$	0.307	0.653
Na^+	$mg\ L^{-1}$	7.16	91.9
Ca^{2+}	$mg\ L^{-1}$	60.00	91.06
Mg^{2+}	$mg\ L^{-1}$	21.03	32

Table S4. Natural population analysis (NPA) charge populations and condensed Fukui index distribution of CBZ

No.	Atom	Charge (-1)	Charge (0)	Charge (+1)	f+	f0	f-
1	N	1.245313	0.261953	0.220688	-0.04127	-0.51231	-0.98336
2	C	0.387802	0.408193	0.461283	0.05309	0.03674	0.020391
3	C	0.291013	0.345162	0.386326	0.041164	0.04765	0.054149
4	C	1.231068	1.232727	1.224975	-0.00775	-0.00305	0.001659
5	C	-0.08624	-0.11833	-0.087548	0.030786	-0.00065	-0.03209
6	C	-0.157783	-0.15757	-0.146074	0.011493	0.00585	0.000216
7	**C**	-0.125114	-0.0993	-0.106556	-0.00725	0.00927	0.025811
8	C	-0.228398	-0.23008	-0.216805	0.013276	0.00579	-0.00168
9	O	-0.710388	-0.67035	-0.558955	0.111391	0.07571	0.040042
10	**N**	-0.984481	-0.97937	-0.945363	0.034007	0.01955	0.005111
11	**C**	**-0.233085**	**-0.14905**	**-0.094991**	**0.054063**	**0.06904**	**0.084031**
12	C	-0.21308	-0.20539	-0.171512	0.033876	0.02078	0.007692
13	**C**	-0.268866	-0.25014	-0.1584	0.091738	0.05523	0.018728
14	**C**	**-0.223392**	**-0.17078**	**-0.071897**	**0.098882**	**0.07574**	**0.052613**
15	**C**	-0.209742	-0.20173	-0.167263	0.034471	0.02124	0.008008
16	C	-0.282577	-0.23721	-0.162451	0.074762	0.06006	0.045364
17	C	-0.239799	-0.23009	-0.19395	0.036135	0.02292	0.009714
18	C	-0.249377	-0.23469	-0.204212	0.030479	0.02258	0.014686
19	H	0.216487	0.2541	0.348967	0.094867	0.06624	0.037613
20	H	0.198046	0.259182	0.34201	0.082828	0.07198	0.061136
21	H	0.38035	0.37621	0.391641	0.015431	0.00564	-0.00414
22	H	0.33959	0.372801	0.435459	0.062658	0.04793	0.033211
23	H	0.15034	0.244672	0.390324	0.145652	0.11999	0.094332
24	H	0.203614	0.241142	0.342789	0.101647	0.06958	0.037528
25	H	0.18725	0.240764	0.37446	0.133696	0.09360	0.053514
26	H	0.148108	0.239542	0.389244	0.149702	0.12056	0.091434
27	H	0.19228	0.250258	0.338816	0.088558	0.07326	0.057978
28	H	0.169859	0.247138	0.365205	0.118067	0.09767	0.077279
29	H	0.186727	0.238761	0.360565	0.121804	0.08691	0.052034
30	H	0.1751	0.245387	0.354602	0.109215	0.08975	0.070287

REFERENCES

1. Q. Ma, Y. Zhang, X. Zhu and B. Chen, *J. Hazard. Material.*, 2022, **427**, 127890.
2. W. Zhang, M. Li, J. Luo, G. Zhang, L. Lin, F. Sun, M. Li, Z. Dong and X.-y. Li, *Chem. Eng. J.*, 2023, **474**, 145377.
3. Y. Lei, X. Guo, M. Jiang, W. Sun, H. He, Y. Chen, K. Thummavichai, O. Ola, Y. Zhu and N. Wang, *Appl. Catal. B Environ.*, 2022, **319**, 121932.
4. H. Wei, J. Zhao, B. Shang and J. Zhai, *J. Environ. Chem. Eng.*, 2022, **10**, 108532.